

Marginal intermediate statistics in the excited spectra of the $E \otimes (b_1 + b_2)$ Jahn–Teller system

This article has been downloaded from IOPscience. Please scroll down to see the full text article.

2008 J. Phys. A: Math. Theor. 41 155102

(<http://iopscience.iop.org/1751-8121/41/15/155102>)

View [the table of contents for this issue](#), or go to the [journal homepage](#) for more

Download details:

IP Address: 171.66.16.148

The article was downloaded on 03/06/2010 at 06:43

Please note that [terms and conditions apply](#).

Marginal intermediate statistics in the excited spectra of the $E \otimes (b_1 + b_2)$ Jahn–Teller system

E Majerníková^{1,2} and S Shpyrko^{2,3}

¹ Institute of Physics, Slovak Academy of Sciences, Dúbravská Cesta 9, SK-84 511 Bratislava, Slovak Republic

² Department of Optics, Palacký University, Tř. 17. Listopadu 50, CZ-77207 Olomouc, Czech Republic

E-mail: Eva.Majernikova@savba.sk and serge_shp@yahoo.com

Received 25 September 2007, in final form 20 January 2008

Published 2 April 2008

Online at stacks.iop.org/JPhysA/41/155102

Abstract

The long-range spectral density correlations (spectral rigidities $\bar{\Delta}_3(\bar{n})$ and related spectral compressibilities) of the $E \otimes (b_1 + b_2)$ Jahn–Teller model are found strongly nonuniversal with respect to the Hamiltonian parameters and inhomogeneous with respect to the choice of a partial energy segment. However, the partial spectral rigidities exhibit common features: an anomalous linear part for small \bar{n} and a saturation for large \bar{n} . The spectral compressibilities found for the partial spectral segments and averaged over a whole relevant part of the spectrum cumulate close to a well-defined limit pertaining to the semi-Poisson statistics. This is in accordance with similar tendencies revealed in the short-range averaged statistical characteristics of this model investigated in our previous paper (Majerníková and Shpyrko 2006 *Phys. Rev. E* **73** 057202). These features document an inhomogeneous and nonuniversal weakening of level repulsions and nonuniversality of level fluctuations on both long and short energy scales. The nonuniversality and inhomogeneity of the statistical characteristics correspond to a similar behaviour of the chaoticity parameter (a fraction of the chaotic phase space of the trajectories) found for the corresponding semiclassical Hamiltonian. We ascribe the nonuniversal and inhomogeneous nonintegrability behaviour to the changing degree of the brokening of the rotation symmetry when changing parameters of our effectively two-dimensional model. It results in a random distribution of the respective localized wavefunctions at all scales up to the size of an available state space. The multifractal behaviour of the wavefunctions is implied from the analysis of their (averaged) fractal dimensions which range up to 1.5 ± 0.1 (for \bar{D}_2). This might imply the concept of the chaos-assisted tunnelling between the regions of reduced degree of stochasticity through regions of high degree of stochasticity. It supports the analogy with the two-dimensional

³ On leave from the Institute for Nuclear Research, Ukrainian Academy of Sciences, pr. Nauki 47, Kiev, Ukraine.

Anderson model with marginal-asymptotically far metal–insulator transition. The features found allow us to classify the present model as a member of the class with a multifractal eigenfunction statistics characteristic for the spectra with weakened level repulsion similar to the Anderson model close to the metal–insulator transition.

PACS numbers: 05.45.–a, 31.30.–i, 63.22.+m

(Some figures in this article are in colour only in the electronic version)

1. Introduction

Investigations of a wide class of complex Hamiltonians show a coexistence of ordered and more disconnected chaotic dynamic regions in their phase space in a semiclassical limit [2]. Respective parameters, fractions of the regular and chaotic regions of the phase space were used for the evaluation of statistical characteristics of the related quantum spectra. Namely, explicit formulae for the nearest-neighbour level spacing distributions [3] and the averaged level number variances or the Δ_3 statistics [4, 5] were illustrated by a model of two coupled quartic oscillators. The level repulsion at small level spacings was shown to be reduced by the fractionating of the chaotic region which substantially complicated related numerical calculations (level spacing distributions). Discrepancies between the numerical data and the analytical formulae for the above-mentioned short-range and also the middle and long-range fluctuation statistics were ascribed especially to quantum effects like the tunnelling between regular regions through chaotic barriers and the quantum interference effects. Finally, the chaos-assisted tunnelling approach to the calculation of the level repulsion implied the correct behaviour of the level spacing distributions in the limit of small level separations [6]. This kind of tunnelling was shown to be connected with the fractal dimension of a two-dimensional phase space due to a hierarchical phase space structure of a chaotic system [7].

In this paper, we try to show that one of the systems which exhibit fluctuation properties typical for a transition region between order and chaos with varying (nonuniversal) degree of nonintegrability is the $E \otimes (b_1 + b_2)$ Jahn–Teller (JT) model. The model is represented by two degenerate electron levels coupled to two phonon (vibron) modes via two different interaction strengths. Unitary diagonalization of the Hamiltonian in the electron space transforms the system onto two highly nonlinearly coupled quantum oscillators in two dimensions.

In a recent paper [1], we have initiated the study of the statistical evidence of quantum chaotic patterns emerging in this model. We have shown that the (short-range) statistics of the nearest-neighbour level spacings (NNS) in the range of interaction parameters apart from the particular symmetry cases ($E \otimes e$ JT and exciton model) is nonuniversal and tends to a well-defined limit close to the semi-Poisson law $P(S) = 4S \exp(-2S)$. This intermediate statistic between the Poisson (uncorrelated levels) and the Wigner–Dyson distribution of a correlated fully chaotic level system was found within the frame of random matrix theory as a critical distribution in the metal–insulator transition region in the Anderson model of disorder [8, 9] as well as in several models with not fully developed chaotic dynamics by Bogomolny [10]. Namely, the semi-Poisson distribution of the level spacings in the plasma model was ascribed to the screening (restriction to a finite number of nearest neighbours) of the logarithmic pair interaction potential. Statistical methods for energy levels and eigenfunctions of disordered systems were reviewed by several authors [11].

In section 2, we shall concentrate on the complementary item of the long-range statistics for the excited spectra of the $E \otimes (b_1 + b_2)$ JT model with broken rotation symmetry. It comprises the spectral rigidity measure of correlations of the level density on scales large when compared to the mean level spacings. Among possible variants of this measure one can cite the $\bar{\Delta}_3$ statistics of Dyson and Mehta [8, 9, 12, 13]. Namely, the Δ_3 value is defined as a (random) quantity which for a given energy interval $[-L, L]$ around the value E_0 gives the deviation of the least-square linear fit line from the staircase function $N(E)$ of the number of levels with energy below E :

$$\Delta_3(L) = \min_{A,B} \left\{ \frac{1}{2L} \int_{-L}^L [N(E) - AE - B]^2 dE \right\} \quad (1)$$

(here the energy is shifted so that the interval is centred around 0; the minimalization is performed with respect to parameters A, B). The average of this measure over ensemble $\bar{\Delta}_3$ is the quantity of the present interest. The $\bar{\Delta}_3$ measure and the correlation function of the level number $\Sigma_2(\bar{n}) \equiv \langle \delta^2 N \rangle = \langle N^2 \rangle - \langle N \rangle^2$ (fluctuations of the level number in an energy band of a width E , $\bar{n} \equiv \langle N \rangle$ is the length of the energy interval measured by the mean number of the levels inside) are related straightforward as $\bar{\Delta}_3(\bar{n}) = \frac{2}{\bar{n}^4} \int_0^{\bar{n}} (\bar{n}^3 - 2\bar{n}^2 r + r^3) \Sigma_2(r) dr$ [14]. The use of the $\bar{\Delta}_3$ -statistics instead of the level number fluctuations Σ_2 is justified by the fact that its variance is suppressed when compared to that of $\langle \delta^2 N \rangle$ [12].

The random matrix theory (RMT) predicts the scaling of this measure as $\log \bar{n}$ (or $\log E$) for the domain of fully developed chaos, meanwhile for the completely uncorrelated sequences of levels a linear scaling $\sim \bar{n}$ is expected [10, 15].

For the Poisson ensemble of an uncorrelated sequence of levels one has $\Sigma_2(r) = r$ and $\bar{\Delta}_3(\bar{n}) = \bar{n}/15$. The number variance $\Sigma_2(\bar{n})$ was calculated for a set of ensembles within RMT supposed to model the behaviour of Anderson-type systems [15, 16]. Its asymptotic form was shown to be similar to the uncorrelated case but with the coefficient (level compressibility) $\chi < 1$, $\Sigma_2(\bar{n}) \sim \chi \bar{n}$ for large \bar{n} . The value $\chi > 0$ at weakened level repulsion (compared to the metallic limit) refers to the fractal nature of wavefunctions. Restricting to the nearest-neighbour interactions of the logarithmic pair potential in the Coulomb plasma model Bogomolny *et al* [10] found the value of the compressibility $\chi = 1/2$ which should hold for the models with the semi-Poisson statistics.

In section 3, we discuss a completing semiclassical concept of the degree of chaoticity, i.e., of the phase space fraction occupied by the chaotic trajectories μ for different segments of the spectra and interaction parameters. A broad region of μ from increasing to maximum values in the low and middle parts of the spectra to the decreasing again values in the upper parts of the spectra occurs, strongly depending on the parameters and location of the spectral segment. These results confirm the nonuniversality and varying nonintegrability properties as obtained in section 2.

In section 4, an independent quantitative statistical analysis of quantum chaotic patterns of long-range type is provided by the fractal properties of the eigenfunctions: the set of fractal dimensions D_q is defined by the scaling properties of the inverse participation ratios $I_q(n)$ related to the eigensolution of the state n of a Hamiltonian as $I_q(n) = \sum_r |\Psi_n(r)|^{2q}$. For the sake of application to the excited states of our electron–vibron model (defined in section 2) it is suitable to use the spectral representation where the relevant substrate is the space spanned by the vibron (phonon) Fock states n [17]:

$$I_q(n) \equiv \sum_i |C_{in}|^{2q}. \quad (2)$$

Here, $C_{in} \equiv \langle \Phi_i | \chi_n \rangle$; $\chi_n(Q_1, Q_2)$ are the exact (numerically calculated for the present model) vibron wavefunctions in the space of coordinates Q_1 and Q_2 ; the base set Φ_i is chosen as

the set of vibron Fock states—excited states i of the unperturbed two-dimensional harmonic oscillator, namely, i is a compound index denoting the direct product of the excited states s and t of the vibrons 1 and 2: $|i\rangle \equiv |s\rangle_1 \otimes |t\rangle_2 \sim b_1^\dagger b_2^\dagger |0\rangle_1 \otimes |0\rangle_2$.

The scaling with the fractal dimension D_q in the spectral representation assumes that one explores the probabilities $P_{i,L}(n) = \sum_{s \in i} P_s(n) = \sum_s C_{s \in i, n}^2$, where the sum is taken over the states inside the cube i of dimension 2 comprising l^2 base Fock states and L denotes the number of these cubes ($L \sim 1/l^2$). Then,

$$I_{q,L}(n) \propto \sum_i^L P_{i,L}^q(n) \propto L^{-D_q(q-1)}, \quad (3)$$

where the information dimension D_1 is understood as usual in the limit $q \rightarrow 1$ as the scaling factor of $\exp(-\sum P_i \log P_i) \propto L^{D_1}$. A common assertion found by Kravtsov and Muttalib [18] states that the critical statistics in certain class of systems including the Anderson model at M–I transition is in an intimate relation with the weakly overlapping (implying multifractality) wavefunctions.

2. $\bar{\Delta}_3$ statistics as a measure of spectral rigidity of the $E \otimes (b_1 + b_2)$ Jahn–Teller model

The $E \otimes (b_1 + b_2)$ JT model is defined by the Hamiltonian

$$\hat{H} = \Omega(b_1^\dagger b_1 + b_2^\dagger b_2 + 1)I + \alpha(b_1^\dagger + b_1)\sigma_z - \beta(b_2^\dagger + b_2)\sigma_x \quad (4)$$

described, e.g., in our previous papers [1, 17, 19]. In short, the local spinless double degenerate electron level is linearly coupled to two intramolecular vibron (phonon) modes of the frequency Ω by different coupling constants $\alpha \neq \beta$. The pseudospin notation with 2×2 Pauli matrices σ_x, σ_z and unit matrix I refers to the two-level electron system. The operators b_i, b_i^\dagger satisfy boson commutation rules $[b_i, b_j^\dagger] = \delta_{ij}$ and define the vibron coordinates $Q_i = (b_i^\dagger + b_i), i = 1, 2$. The interaction term $\alpha\alpha$ removes the degeneracy of the electron levels and the term $\alpha\beta$ mediates the vibron-assisted electron tunnelling between the levels (the class of exciton models differs from the present one by the absence of the vibron-2 assistance in the tunnelling term $\sim\beta$). Two cases of special symmetry comprise the rotation symmetric $E \otimes e$ JT model ($\alpha = \beta$) and the polaron model with $\beta = 0$ or $\alpha = 0$. Introducing nonequal coupling constants the model above generalizes the common $E \otimes e$ Jahn–Teller model. The interest for such a generalization has various sources, in particular: (a) different coupling constants are likely to be caused by a spatial anisotropy in a crystal plane; (b) two vibron modes need not have necessary the same frequencies. In this case, the Hamiltonian can be appropriately rescaled to the present model with equal frequencies but different coupling strengths (in what follows we set $\Omega = 1$); and, last but not least, (c) the generalized JT system with broken rotational symmetry presents more rich variety of generic chaotic properties than its simpler prototype. As it was shown [1, 17] it stands closer to the generic models of quantum chaotic behaviour.

In the following, we use the vibron eigenfunctions of the transformed Hamiltonian $\tilde{H} \equiv U \hat{H} U^{-1}$ [17, 19]

$$\tilde{H} = \Omega \left(\sum_{i=1,2} b_i^\dagger b_i + 1 \right) + \alpha(b_1^\dagger + b_1) - p\beta(b_2^\dagger + b_2)R_{\text{ph}} \quad (5)$$

exactly diagonalized in the electron subspace by the Fulton–Gouterman (FG) unitary operator $U = \frac{1}{\sqrt{2}} \begin{pmatrix} 1 & R_{\text{ph}} \\ 1 & -R_{\text{ph}} \end{pmatrix}$, where $R_{\text{ph}} = \exp(i\pi b_1^\dagger b_1)$ is the vibron reflection operator imposing high nonlinearity in the system and the parity $p = \pm 1$. It is easy to see that in the FG

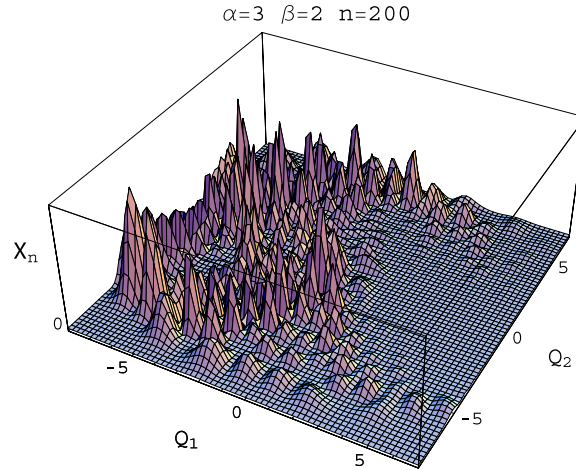


Figure 1. Example of the wavefunction $\chi_n(Q_1, Q_2)$ for $\alpha = 3, \beta = 2$ and $n = 200$.

representation the parities $p = \pm 1$ are exactly mirror images of each other and can be mapped one onto another by a mere change of the sign in the definition of the phonon-2 displacements ($\hat{Q}_2 \rightarrow -\hat{Q}_2$), thus the system remains doubly degenerated and the parity does not have any impact on the properties of the spectrum; in what follows we choose $p = +1$.

In the representation of radial coordinates in the plane $Q_1 \times Q_2$, $Q_1 = r \cos \phi$, $Q_2 = r \sin \phi$, the transformed Hamiltonian (5) yields [17]

$$\tilde{H} = -\frac{1}{2r} \frac{\partial}{\partial r} \left(r \frac{\partial}{\partial r} \right) + \frac{1}{2} r^2 - \frac{1}{2r^2} \cdot \frac{\partial^2}{\partial \phi^2} + \sqrt{2}\alpha r (\cos \phi - \sin \phi R_{\text{ph}}) I + p\sqrt{2}(\alpha - \beta)r \sin \phi R_{\text{ph}}. \quad (6)$$

The reflection operator R_{ph} in radial coordinates acts as $R_{\text{ph}}(r, \phi) f(r, \phi) = f(r, \pi - \phi)$ on some $f(r, \phi)$. An example of the numerical eigenfunction to the transformed Hamiltonian (5) in the space $Q_1 \times Q_2$ is shown in figure 1. Let us note the apparent fractal nature of the space distribution of the state amplitude⁴. The Hamiltonian (6) commutes with the operator of the angular momentum $\hat{J} = i(b_1 b_2^\dagger - b_1^\dagger b_2) - \sigma_y/2$ if $\alpha = \beta$. Thus, the eigenfunctions of the symmetric model can be chosen each to pertain to a state with a good quantum number $|j| = 1/2, 3/2, \dots$ [17].

The last term in (6) breaks the rotational symmetry and involves interactions of the basis states with different j . Hence, a wavefunction of the full Hamiltonian is now distributed over a range of values of the angular momentum (figure 2). An analogy to the two-dimensional Anderson model of disorder can be traced if the base functions with definite j are considered as ‘pseudositers’ over which the wavefunction is spread. Similarly as in the Anderson model, the properties of the model are determined by the relative strengths of the intersite (different j) and the onsite interactions. The microscopic reason for this analogy is the assistance of phonons-2

⁴ It is to be noted that the energy spectrum of the system is invariant with respect to the interchange $\alpha \leftrightarrow \beta$. But the system itself is not invariant with respect to this interchange. For example, the ground state is essentially different in the domains of heavy ($\alpha > \beta$) and light ($\alpha < \beta$) polarons [19]. However, in the Fock state representation the components of the corresponding wave vectors differ up to the sign change which does not affect the fractal properties of wavefunctions in the spectral representation and, hence, the symmetry of exposed results with respect to the said transformation.

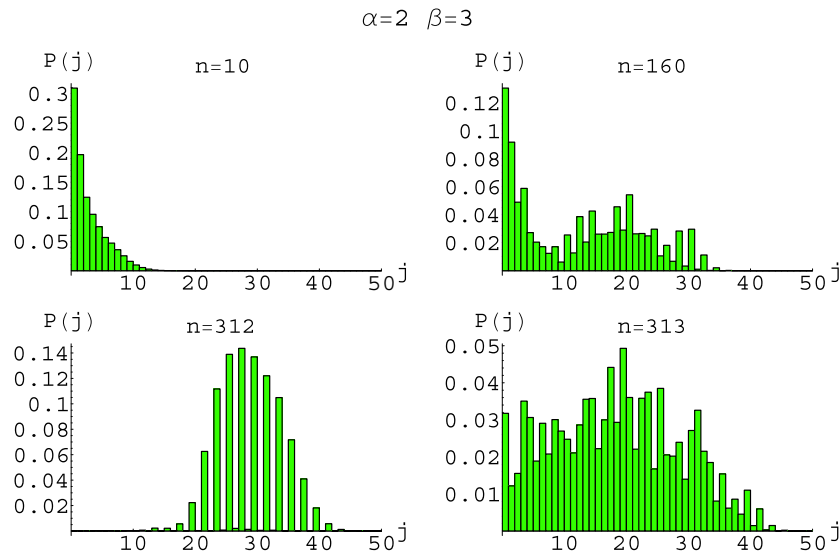


Figure 2. Examples of distributions of wavefunctions over j -space for $\alpha = 2, \beta = 3$. Evidently, the states exhibit different extent of localization.

in transitions between the levels (6) which allows for the emerging of the pseudolattice. In our opinion, it is just these transitions with changing symmetry (R_{ph}) which ensured the similarity of the results for NNS distribution [1] to the Anderson model close to the M–I transition (marginal in two dimensions). Traces of quantum chaos cause the sequence of these coefficients to be distributed in a random fashion with varying n thus supporting the analogy to the Anderson model with *a priori* given random coefficients.

Calculating the angular part of the matrix elements of the symmetry breaking term in (6) between the states of the harmonic oscillator the selection rules can be obtained which assert that the element with definite j is directly connected to the elements with $j' = j + 2, j - 2$ (cf especially figure 2 with $n = 312$ where only every odd ‘pseudosite’ j is populated). This reminds us of an analogy with the ‘daisy models’ of random matrix ensembles [20] with dropping every second level which was shown to lead directly to the semi-Poisson distribution of NNS. The natural ‘length’ of our pseudolattice (for a given interval of energy) is thus the maximal number of allowed values of angular momentum for a given n (level number), that is $L \sim \sqrt{n}$ (a state with main quantum number $n_r = 0, 1, \dots$ of a two-dimensional harmonic oscillator is $n_r + 1$ times degenerated with an auxiliary quantum number ranging between 0 and n_r , hence $n \sim n_r^2$). Thus, the analogy to the Anderson-type models with M–I transition whose intrinsic characteristics is the length L of a system appears now more pronounced.

In order to calculate the long-range averaged characteristics of the energy spectra of (5) we numerically diagonalized the Hamiltonian matrix in the representation of the base Fock states of the vibrons 1 and 2. Taking N_1 and N_2 base Fock states for each vibron we introduced an appropriate ordering of sites [21] so that a state vector turned to be a vector with $N_1 \cdot N_2$ elements. Numerical determination of high energy states produces an inevitable error because of truncating the base space. Varying the numbers of the base states we investigated the convergence of the results. For practical purposes we limited ourselves by the base size $N_1 \times N_2 = 75 \times 75$ from whence about 1100–1200 states appeared to be trustworthy (giving the convergence up to $0.1 \times (\text{characteristic level spacing})$). This number of energy levels was

used in the following calculations. Thus, the obtained spectrum needs to be unfolded in order to ensure its homogeneity (that is normalized so that the local averaged level spacing is unity). To do so it is necessary to fit the ‘staircase’ $N(E)$ (or the corresponding level density $\rho(E) = \sum_i \delta(E - E_i)$) by a reasonably chosen smooth function. Different choices of the latter are possible. The calculations below used the unfolding by fitting the level density by a third-order spline polynomial (after smoothing the data via Gaussian smoothing with the smoothing constant 0.3) in the domain of interest, that is for level numbers 100–1200. In this interval the level density of our two-vibron system grows almost linearly with the energy (we note in passing that this behaviour is in a qualitative accordance with the semiclassical Weyl formula giving generically a linear growth of the level density for a two-vibron system), so that such fitting turns to be more than satisfactory. We performed sample calculations with an increasing order of polynomials, and using other algorithms of producing the smoothed level density ρ_{sm} as well (in particular, varying the parameters of the Gaussian smoothing and using the smoothing via moving average/median); the results appeared indistinguishable within statistical errors.

In order to compile a statistical ensemble out of the (deterministic) quantum problem one has to perform averaging of the numerical quantities of interest over different parts of the spectrum taken as members of this ensemble. We included into the statistical analysis the energy intervals centred at different starting values ranging between 100 and 1100 levels which corresponded to the energy values between (-10) and (-5) and between 25 and 30 depending on the values of (α, β) . However, as it follows from the results below, the ensemble averaged properties can show a bias (sensitivity to the starting point in the energy range), therefore this procedure must be followed with maximal care. To improve the statistics we also followed the standard procedure of collecting statistical data from small intervals in the space of parameters (α, β) . To be exact, for a given point of interest (α_0, β_0) we collected the energy values from the square $(\alpha_0, \beta_0) \pm 0.25$ in the parameter space with the step 0.1. (The exception of this rule was collecting the data for the points where $\alpha_0 = \beta_0$. There, this restriction was followed for choosing the neighbouring parameters for the sampling.) From figure 4 it follows that indeed the averaged statistical data present a slight bias when taking different energy intervals. Therefore, we presented the results in figure 4 separately in two energy bins for lower (100–600) and higher (600–1100) levels. It is worth noting that the nonsymmetric parameter values ($\alpha \neq \beta$) appear to present more robust statistics with respect to the energy interval than the symmetric ones ($\alpha = \beta$). The same conclusion was already drawn from the investigation of the short-range statistics [1, 17] where we showed that the spectral properties of the nonsymmetric JT models were more homogeneous with respect to the choice of the energy interval. Taking smaller energy bins than those of figure 4 however did not change much the appearance of the corresponding figures.

In figure 3, the samples of the long-range spectral correlations $\bar{\Delta}_3$ of the U -transformed Hamiltonian (5) (unfolded in a fashion described above) are presented for several sets of interaction parameters. It is seen that the spectral rigidity shows up serious deviations from the Poisson behaviour as well as from the logarithmic dependence expected in the frame of RMT. For large \bar{n} it supposedly tends to a saturation, and a characteristic linear domain is evident for small \bar{n} (up to $\bar{n} \sim 15$).

In figures 4 and 5, we plot the level compressibilities (slopes $d\bar{\Delta}_3(\bar{n})/d\bar{n}|_{\bar{n}=0}$ of the $\bar{\Delta}_3$ curves) for a range of parameters α, β . The slopes in figures 4(a) and (b) were calculated from averaging over 500 levels in the ranges 100–600 and 600–1100, respectively. Taking lower levels would bring us below the ‘diabatic line’ where the system fills only one potential well of the ‘effective potential’ (see [17, 19] for a detailed discussion). It is seen from figure 4 that results for different intervals of energy show differences, but, nevertheless, similar tendencies.

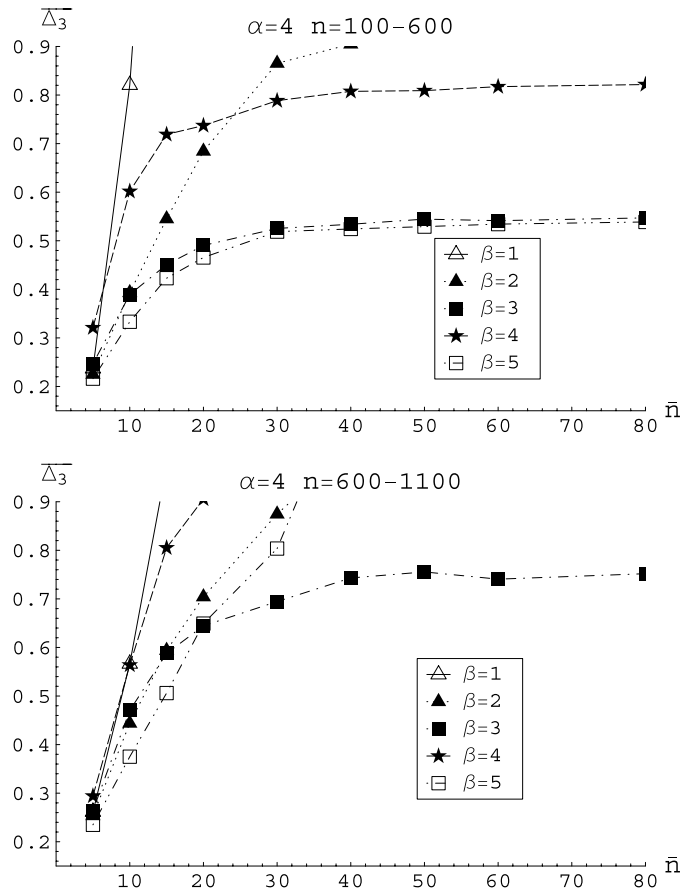


Figure 3. Spectral rigidities ($\bar{\Delta}_3$ -statistics) in different segments of the spectra for the $E \otimes (b_1 + b_2)$ JT model. The slopes are linear for \bar{n} at least up to 15 and tend to nonuniversal saturation values $\bar{\Delta}_{3\max}(\beta)$ for large \bar{n} .

Apart from the cases close to the special symmetries ($\alpha = \beta$ and $\alpha \ll \beta, \alpha \gg \beta$) the slopes show a markable accumulation close to the value $\chi = 0.5/15$ (the horizontal grid line at 0.033) indicating the semi-Poisson limit. This limit is more pronounced at higher levels (interval 600–1100), where even the points corresponding to the symmetric cases $\alpha = \beta$ are close to this line. For lower energy intervals (levels 100–600) this universality is seen less, although all $\bar{\Delta}_3$ curves points are far from both Poisson and RMT limits. For lower energies there is also a more pronounced difference between symmetric and nonsymmetric models: meanwhile the nonsymmetric values of parameters still tend to the semi-Poisson limit, the symmetric points however show essential deviation from this limit towards the Poisson case.

In figure 3, the $\bar{\Delta}_3(\bar{n})/d\bar{n}|_{\bar{n}}$ curves for $\beta = 2, 4$ for $\alpha = 3$ (scaled by $\Omega = 1$) averaged over the whole relevant extent of the spectra (up to the level $n = 1100$) are situated very close one to another, i.e. they are getting close to a limit with the minimal slope.

The said marginality also emerged in the statistics of NNS [1]. We have shown that the dispersions σ^2 of NNS distributions in the range of parameters far from the mentioned special symmetry cases tend to a limit $\sigma^2 \simeq 0.5$ characteristic for the M–I transition of the Anderson model.

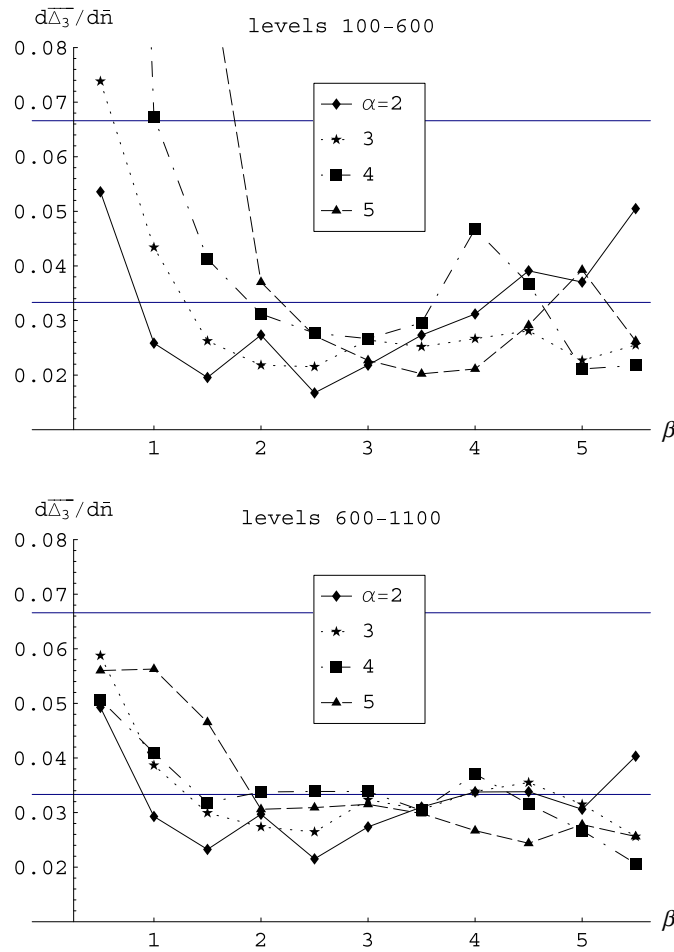


Figure 4. Slopes $d\bar{\Delta}_3(\bar{n})/d\bar{n}|_{\bar{n}=0}$ (‘level compressibilities’) of the long-range statistical measure for different model parameters (α, β) for different parts of the spectra. The grid lines indicate the Poisson line ($1/15$) and the marginal semi-Poisson limit ($\chi = 0.5/15 \simeq 0.033$). The dispersion of the probability distributions pertaining to the displayed mean values is ~ 0.01 . The pictures show a strong dependence on the position of the fragment within the spectra.

3. Quasiclassical description in the phase space

It is interesting to discuss the mapping between the exposed results and the semiclassical description of the same system. The search for the quantum chaotic patterns historically meant looking for quantum correspondence to the chaotic behaviour of the classical trajectories. First of all it is to be noted that the passage to the (semi)classical description in a two- or many-level electron–phonon system can be performed in several fashions. The most straightforward ‘semiclassical’ description of the quantum JT problem is obtained if we pass to the real Bloch variables made of pseudospin Pauli matrices:

$$x(t) := \langle \sigma_x \rangle_t \quad y(t) := \langle \sigma_y \rangle_t \quad z(t) := \langle \sigma_z \rangle_t, \quad (7)$$

and perform the appropriate decoupling of the oscillatory (phonon) and electron variables in the initial Hamiltonian (4) within the framework of the Born–Oppenheimer approximation:

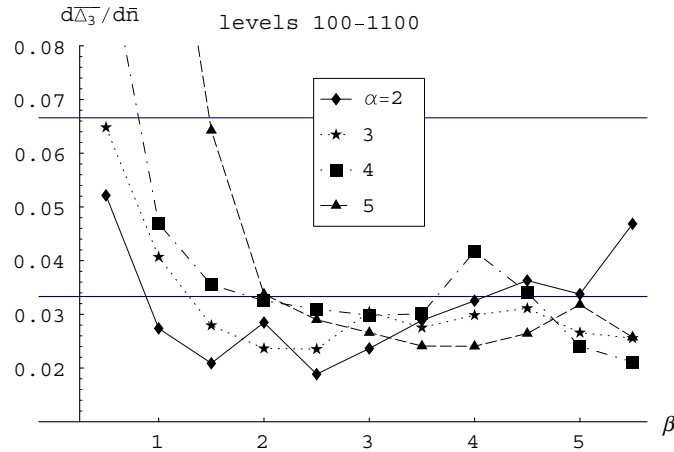


Figure 5. The cumulative slopes $d\bar{\Delta}_3(\bar{n})/d\bar{n}|_{\bar{n}=0}$ averaged over the relevant extent of the spectra. Large deviation of the points $\alpha = 4, \beta > 4$ from the suggested marginal line is explained by their relative proximity to the symmetric point $\alpha = \beta = 4$.

$\langle \hat{Q}_1 \hat{\sigma}_x \rangle \rightarrow \langle \hat{Q}_1 \rangle(t)x(t)$, etc. Another way of passing to the semiclassical description follows from the form of the Hamiltonian (5) where the electron degrees of freedom are exactly eliminated at the cost of the strongly nonlinear coupling of the phonon degrees of freedom. The semiclassical decoupling then means the decoupling of the vibrons 1 and 2. The classical equations of motions in this variant are implied by the following classical Hamiltonian as a function of the coordinates γ_i and respective momenta π_i :

$$H(\gamma_1, \pi_1, \gamma_2, \pi_2) = \frac{1}{2}[\pi_1^2 + \pi_2^2 + \gamma_1^2 + \gamma_2^2] + \alpha\gamma_1 \mp \beta\gamma_2 \exp(-2(\gamma_1^2 + \pi_1^2)). \quad (8)$$

The trivial linear stability analysis shows that the stationary point $(\gamma_1, \gamma_2, \pi_1 = \pi_2 = 0)$ is unstable unless $\alpha \gg \beta, \alpha \ll \beta$ or unless the parameters (α, β) are located in the small domain near the point $\alpha = \beta = 0$. The crucial characteristics of interest is however the chaoticity of the phase space, in particular, its fraction μ occupied by the chaotic trajectories. The formulae which relate this quantity to the parameters of the statistics of quantum levels for both short- and long-range statistics are widely known [3–5]. We investigated the chaoticity of the trajectories implied by the Hamiltonian (8) and performed rough estimations of the ‘chaoticity parameter’ μ for different energies. We studied the sensitivity of the classical equations of motion to the initial conditions checking whether two initially neighbouring trajectories diverge in the course of time (that is studying the Lyapunov index [4, 5, 22]). The fraction of the chaotic trajectories at given energy E was then estimated by taking at random the initial points respecting $H(\gamma_1, \pi_1, \gamma_2, \pi_2) = E$. The detailed quantitative presentation of this work is to be given elsewhere; for the sake of the present contribution we just mention the results briefly. The classical phase space in the energy range corresponding to the energies of quantum levels used (that is up to $E \sim 30$) appears to be pronouncedly chaotic. The fraction of chaotic levels increases rapidly with the increase of energy and reaches its maximum $\mu \sim 0.90\text{--}0.99$ for the energies typically $E \sim 10$ which roughly corresponds to the lower energy bin of figure 4 (levels 100–600). With further increasing energy the value of μ then slowly decreases. Its estimations for E between 20 and 30 range from 0.3 to 0.75 strongly depending on the parameters α and β . This latter energy interval approximately corresponds to the higher energy bin of figure 4(b). We note once again the more pronounced universality

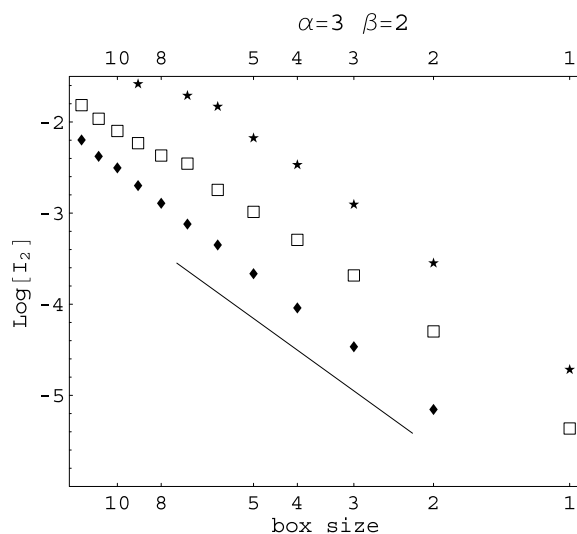


Figure 6. Examples of scaling of the inverse participation ratio $I_2(n)$ as a function of the box size l in the box-counting algorithm as the illustration of the reliability of the scaling (3) for our model. Different shapes of symbols correspond to the values for different levels n : diamonds for $n = 153$, stars for $n = 157$ and squares for $n = 161$. The domain of linear slopes (proportional to the fractal dimensions D_2) extends up to the box sizes $\sim 8 \times 8$ (at larger box sizes the linearity is violated due to the size effects). Slight level-to-level fluctuations of the slopes are also seen. Similar scaling can be demonstrated for $q = 3, 4$ as well.

of the quantum characteristics at the upper bin (figure 4(b)) which appears to correspond to the moderate values of the degree of the classical chaoticity. The quantitative conclusions for this item is however a challenge for a separate study.

In any case, the above results confirm the nonuniversal degree of the classical nonintegrability demonstrated by the dependence of the chaoticity parameter μ on the model parameters α and β and on the location of the energy segment in the spectra. Moreover, the linear dependence of the spectral rigidities in certain parts of the spectra implies a strong suppression of the level repulsions because of the presence of regions with various degree of chaoticity and related chaos-assisted tunnelling between the regions of small degrees of chaoticity. Analogous nonuniversal behaviour of the level compressibilities presented in figure 4 indicates a cumulation of most of their values in the chaotic region $(0, 0.033)$ close to the semi-Poisson values $0.5/15$ depending on the spectral segment where the chaoticity parameter is correspondingly reduced.

4. Fractal dimensions and multifractality of the JT-excited wavefunctions

An independent quantitative analysis of the properties of the $E \otimes (b_1 + b_2)$ excited spectra can be obtained by exploring the scaling of the inverse participation ratio (2) and (3) in the spectral representation of Fock states and following calculation of related fractal dimensions. In figure 6, we give the samples of the scaling of $\log I_{2,L}(n)$ (from equation (3)) for several successive states as functions of the box size l ($L \sim 1/l^2$) comprising l^2 Fock states. The linear slope in the log–log coordinates stretches up to the box sizes 8×8 which indicates the existence of a well-determined quantity D_2 for each level, although the generalized fractal dimensions show slight level-to-level fluctuations.

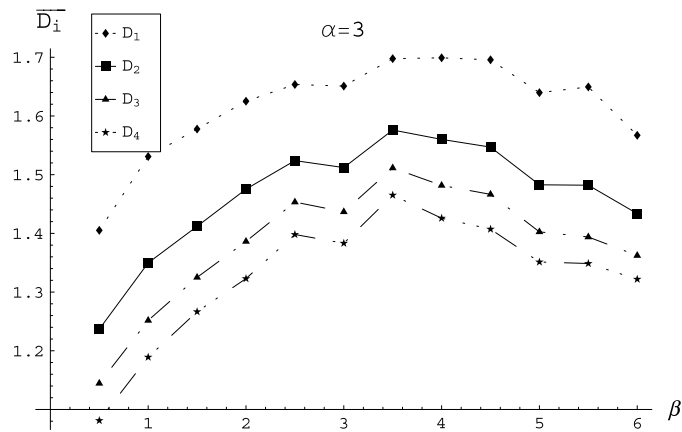


Figure 7. Fractal dimensions \bar{D}_q averaged over n for different pairs of $\alpha = 3, \beta$. A weak multifractality is evident when comparing \bar{D}_q for different q .

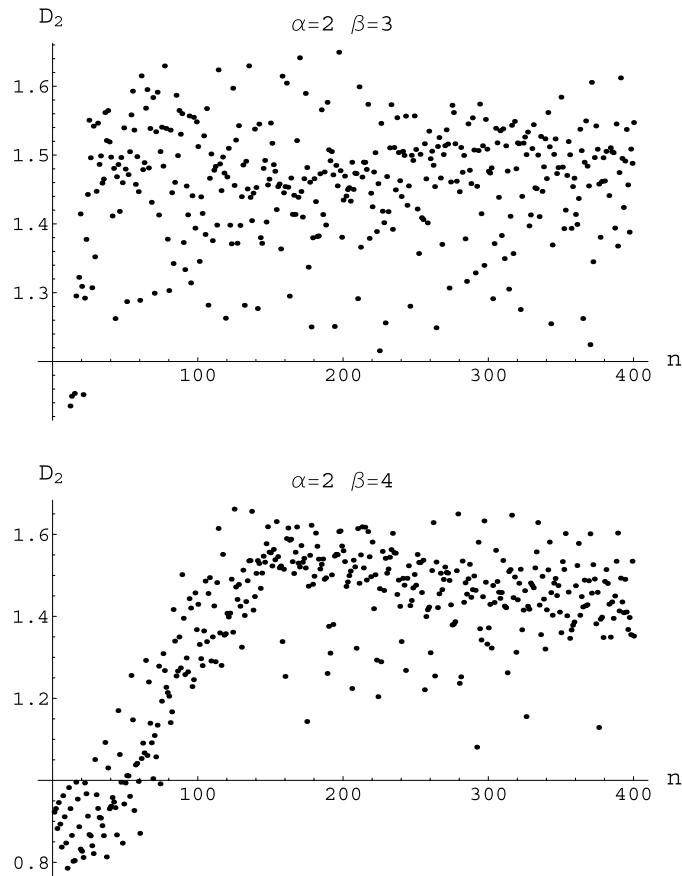


Figure 8. Fluctuations of fractal dimensions D_2 over levels n for different pairs α, β .

In figure 7, the averaged fractal dimensions $\bar{D}_q, q = 1, 2, 3, 4$, in the spectral representation are displayed for a set of interaction strengths. Small variations of \bar{D}_q ($\bar{D}_i < \bar{D}_j$

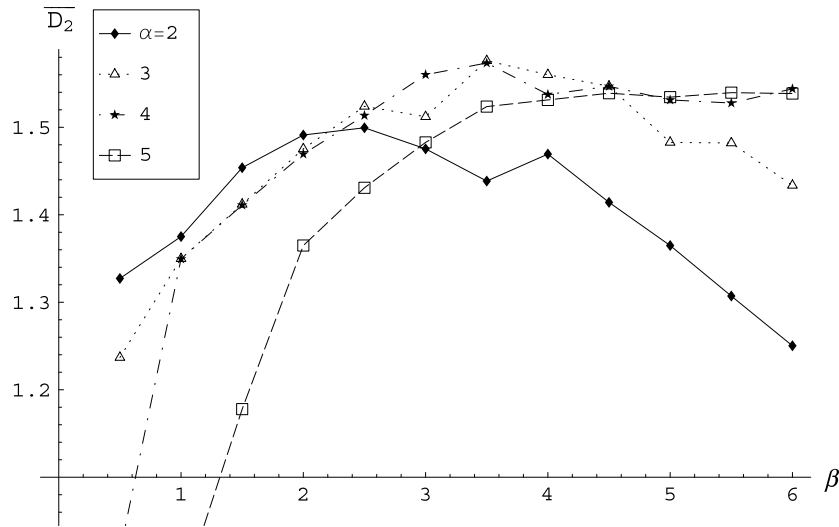


Figure 9. Fractal dimensions \bar{D}_2 averaged over n in the range 200–400 for different pairs α, β . In the ‘most chaotic’ domain the values of \bar{D}_2 are distributed in a narrow region $\sim 1.5 \pm 0.1$.

at $i > j$) testify a weak multifractality of the respective wavefunctions. The fractal dimensions D_q show strong fluctuations with changing n (figure 8) so that one has to speak rather about their statistical distributions [23]. It is seen that this distribution may have a pronounced drift—there occurs a crossover between dimensions $d = 1$ and $d = 2$ at low n . It becomes more homogeneous when n increases. In view of the interpretation in terms of the 1D ‘pseudolattice’ in j -space with natural size of the order $\sim \sqrt{n}$ this can be understood as a tendency towards a universal distribution in the limit of a very large lattice size. Such a limiting behaviour of statistical characteristics of the distribution of fractal dimensions for large lattice sizes of the Anderson model at M–I transition was conjectured by Parshin *et al* [23].

Despite the level-to-level fluctuations of the fractal dimensions (figure 8) their values averaged over level numbers appear to exhibit marginal universality in a similar sense as the universality marked in figure 4. The averaged fractal dimensions \bar{D}_2 in figure 9 show a remarkable tendency to values 1.5 ± 0.1 apart from the case $\alpha \gg \beta$ or $\alpha \ll \beta$.

5. Conclusion remarks

The statistical properties of the investigated JT model are closely related to its spatial symmetry given by the interaction strengths α, β . Our numerical analysis of the spectral rigidity, its slopes and fractal dimensions bring the evidence for their apparent nonuniversality and spectral inhomogeneity. Namely, our results allow us to conclude that the nonuniversality is related by the dimensional crossover between $d = 1$ and $d = 2$ when changing the parameters α, β . A support for this suggestion is the behaviour of the fractal dimension \bar{D}_2 (figure 9) which approach very close to the value 1.5 at the points $\alpha = \beta$. In the neighbourhood of this point the nonuniversality of \bar{D}_2 is the most moderate; the deviations from 1.5 extend within the interval ± 0.1 .

We have shown that although the long-range correlation measure $\bar{\Delta}_3(\bar{n})$ and the partial compressibilities (averaged over partial segments of the spectra) are nonuniversal and highly

inhomogeneous, the slopes *averaged over the whole relevant spectra* approach marginally (quantitatively close) to the universal value characteristic for the semi-Poisson distribution, $0.5/15 \sim 0.033$. This behaviour is analogous to the well-defined marginal behaviour of the average fractal dimensions \bar{D}_2 of the respective wavefunctions mentioned above. To our knowledge, till now the theory justifying the existence of the limiting ‘universal’ value related to the said distribution is lacking. The only relation $\chi = (d - D_2)/2d$ derived by Kravtsov and Lerner [15] was the first bridge between the fractal dimension D_2 and the long-range level statistics. However, it is proven to be valid only for small values of compressibility and does not fit to our calculations.

We have also revealed the corresponding nonuniversal and inhomogeneous behaviour of the chaoticity parameter—the fraction of the chaotic phase space of the classical trajectories. The detailed analysis of this parameter in the whole phase space would be very useful for further considerations of phenomena especially related to the mixing [7] of the phase space between the regions of different degrees of chaoticity. The presence of the mixing phenomena is supported by the multifractal behaviour of the wavefunctions. Because of the nonexistence of the extended states in our model we can conclude on the concept of the chaos-assisted tunnelling between the domains with reduced stochasticity through those with a high degree of stochasticity.

Besides the Anderson model close to the metal–insulator transition [8] other models sharing the universal semi-Poisson statistics are known—in particular, the Bogomolny [10] plasma model with screened Coulomb interactions and the ‘daisy models’ [20].

Acknowledgments

We thank Dr P Markoš for useful discussions. The support of the project by the Grant Agency of the Czech Republic No 202/06/0396 is greatly acknowledged. Partial support is acknowledged also for the Project No 2/6073/26 by the Grant Agency VEGA, Bratislava.

References

- [1] Majerníková E and Shpyrko S 2006 *Phys. Rev. E* **73** 057202
- [2] Bohigas O, Tomsovic S and Ullmo D 1993 *Phys. Rep.* **223** 43
- [3] Berry M V and Robnik M 1984 *J. Phys. A: Math. Gen.* **17** 2413
- [4] Seligman T H and Verbaarschot J J M 1985 *J. Phys. A: Math. Gen.* **18** 2227
- [5] Seligman T H, Verbaarschot J J M and Zirnbauer M R 1985 *J. Phys. A: Math. Gen.* **18** 2751
- [6] Podolskiy V A and Narimanov E E 2003 *Phys. Rev. Lett.* **91** 263601
- [7] Ketzmerick R 1996 *Phys. Rev. B* **54** 10841
- [8] Shklovskii B I, Shapiro B, Sears B R, Lambrianides P and Shore H B 1993 *Phys. Rev. B* **47** 11487
- [9] Evangelou S N and Pichard J-L 2000 *Phys. Rev. Lett.* **84** 1643
Evangelou S N and Katsanos D E 2005 *Phys. Lett. A* **334** 331
- [10] Bogomolny E B, Gerland U and Schmit C 1999 *Phys. Rev. E* **59** R1315
Bogomolny E B, Gerland U and Schmit C 2001 *Eur. Phys. J. B* **19** 121
- [11] Janssen M 1998 *Phys. Rep.* **295** 1
Mirlin A D 2000 *Phys. Rep.* **326** 260
- [12] Dyson F J and Mehta M L 2000 *J. Math. Phys.* **4** 701
- [13] Mehta M L 1960 *Nucl. Phys.* **18** 395
Mehta M L and Gaudin M 1960 *Nucl. Phys.* **18** 420
Gaudin M 1961 *Nucl. Phys.* **25** 447
- [14] Pandey A 1979 *Ann. Phys.* **119** 170
- [15] Kravtsov V E and Lerner I V 1994 *Phys. Rev. Lett.* **72** 888
Kravtsov V E and Lerner I V 1995 *Phys. Rev. Lett.* **74** 2563

- [16] Chalker J T, Kravtsov V E and Lerner I V 1996 *Pis'ma v ZhETF* **64** 355
Chalker J T, Kravtsov V E and Lerner I V 1996 *JETP Lett.* **64** 386
- [17] Majerníková E and Shpyrko S 2006 *Phys. Rev. E* **73** 066215
- [18] Kravtsov V E and Muttalib K A 1997 *Phys. Rev. Lett.* **79** 1913
- [19] Majerníková E and Shpyrko S 2003 *J. Phys.: Condens. Matter* **15** 2137
- [20] Hernández-Saldaña H, Flores J and Seligman T H 1999 *Phys. Rev. E* **60** 449
- [21] Zyczkowski K, Molinari L and Izrailev F M 1994 *J. Phys. I (France)* **4** 1469
- [22] Benettin G and Strelcyn J M 1978 *Phys. Rev. A* **17** 773
Benettin G, Galgani L and Strelcyn J M 1976 *Phys. Rev. A* **14** 2338
- [23] Parshin D A and Schober H R 1999 *Phys. Rev. Lett.* **83** 4590